Evolution of ferromagnetic and non-Fermi-liquid states with doping: The case of Ru-doped UCoGe

Michal Vališka,[1,*] Jiří Pospíšil,[2] Martin Diviš,[1] Jan Prokleška,[1] Vladimír Sechovský,[1] and Mohsen M. Abd-Elmeguid[3]
[1]*Faculty of Mathematics and Physics, Charles University, DCMP, Ke Karlovu 5, CZ-12116 Praha 2, Czech Republic*
[2]*Advanced Science Research Center, Japan Atomic Energy Agency, Tokai, Ibaraki 319-1195, Japan*
[3]*II. Physikalisches Institut, Universität zu Köln, 0937 Köln, Germany*
(Received 29 December 2014; published 14 July 2015)

We have investigated the impact of Ru substitution for Co on the behavior of the ferromagnetic superconductor UCoGe by performing x-ray diffraction, magnetization, specific heat, and electrical resistivity measurements on polycrystalline samples of the $UCo_{1-x}Ru_xGe$ series ($0 \geqslant x \leqslant 0.9$). The initial Ru substitution up to $x \approx 0.1$ leads to a simultaneous sharp increase of the Curie temperature and spontaneous magnetization up to maximum values of $T_C = 8.6$ K and $M_S = 0.1\mu_B$ per formula unit, respectively, whereas superconductivity vanishes already for $x \approx 0.03$. Further increase of the Ru content beyond $x \approx 0.1$ leads to a precipitous decrease of both T_C and M_S towards a ferromagnetic quantum critical point (QCP) at $x_{cr} = 0.31$. Consequently, the $T - x$ magnetic phase diagram consists of a well-developed ferromagnetic dome. We discuss the evolution of ferromagnetism with x on the basis of band structure changes due to varying $5f$-ligand hybridization. This scenario is supported by the results of electronic structure calculations and consideration of the simplified periodic Anderson model. The analysis of the temperature dependencies of the electrical resistivity and heat capacity at low temperatures of the samples in the vicinity of the QCP reveals a non-Fermi-liquid behavior and assigns the ferromagnetic quantum phase transition to be most likely of a continuous Hertz-Millis type.

DOI: 10.1103/PhysRevB.92.045114 PACS number(s): 71.10.Hf, 74.40.Kb, 71.20.Lp

I. INTRODUCTION

The phenomena emerging near a quantum critical point (QCP) belong to the most intensively studied topics of condensed matter physics. Diligent research in this field continuously brings brand new materials carrying completely novel properties. Such progress boosts development of new theoretical approaches describing electron correlations in these systems. A specific group of those intriguing materials comprises the uranium based ferromagnetic superconductors (FM SC) UGe_2 [1,2], URhGe [3], and UCoGe [4]. In these compounds superconductivity (SC) and itinerant ferromagnetism (FM) are carried by the same uranium $5f$ electrons. It is a novelty distinguishing them from previously reported $ZrZn_2$ [5]. UGe_2, the first discovered case, is a model example of SC induced by external pressure. Here SC appears and reaches a maximum T_{SC} on a boundary between two different FM phases under high pressure. URhGe and UCoGe are ambient pressure FM SC where both phenomena naturally coexist. A lot of effort both in theory and experiment has been made to explore the underlying mechanisms of the coexistence of FM and SC. FM spin fluctuations which appear in the vicinity of the QCP have been considered as the main essence for inducing the unconventional spin-triplet SC state [6–8].

Quantum phase transitions (QPTs) were experimentally studied for a broad spectrum of materials such as high-T_C SCs [9], ordinary metals [10], or heavy-fermion compounds [11]. Most of such investigations have been carried out on antiferromagnets which by rule exhibit second-order QCP. Prominent examples are $CeCu_{6-x}Au_x$ with an antiferromagnetic quantum critical point (AF QCP) which is induced by chemical doping [12] or $YbRh_2Si_2$ where the AF QCP is achieved by applying an external magnetic field [13]. Studies of quantum criticality in FMs have been less frequent and manifest that here the situation may be much more complex. The FM phase transition at finite Curie temperature (T_C) is by rule of a second-order type. T_C of itinerant electron FMs is often easily suppressed to 0 K by external pressure p or chemical composition x. However, detailed experimental investigation of archetypal FM metals such as MnSi [10], $ZrZn_2$ [5], or UGe_2 [2,14] has revealed that the FM phase is suppressed to zero temperature at a first-order transition, which would mean that no QCP is observed. This can be elucidated theoretically either in terms of additional fermionic modes which may couple to the critical FM fluctuations driving the phase transition to a first-order type [15], or that a first-order magnetic phase transition may be induced by strong magnetoelastic coupling [16]. No generic scenario can be drawn for the QPTs of the above mentioned materials because of rather individually different phenomena appearing in the quantum critical region. In particular, MnSi becomes long-period helimagnetic (showing FM only locally) in which the thermal phase transition is weakly first-order [17], UGe_2 exhibits strong uniaxial anisotropy [18] and $ZrZn_2$ exhibits a marginal Fermi-liquid ground state [19].

UCoGe, the subject of the present study, is unique in the group of FM SC due to the much lower energy scale on which the magnetism appears [20]. The low T_C of UCoGe of only 3 K [4,21] together with the tiny spontaneous magnetization of $0.03\mu_B$ per formula unit (f.u.) indicate that UCoGe is close to a FM instability [22]. It has been observed, however, that the Ru and Fe substitution for Co rapidly stabilizes the FM state [23], despite the fact that URuGe and UFeGe behave like Pauli paramagnets down to the lowest temperatures [24]. A similar increase of T_C was reported in the case of the initial substitution of Co and Ru for Rh in URhGe [25,26] with the development of a non-Fermi-liquid (NFL) state on the higher doping boundary of the FM dome [26]. These observations motivated us to inspect the development of the magnetic as well as electrical and thermal transport properties

*michal.valiska@gmail.com

in the $UCo_{1-x}Ru_xGe$ series over the entire concentration range ($0 \geqslant x \leqslant 0.9$). Our study is based on extensive investigation of the crystal structure, magnetization, ac magnetic susceptibility, specific heat, and electrical resistance of numerous polycrystalline samples with various Ru content. The results are discussed and compared with theoretical calculations and related models considering the leading role of the $5f$-ligand hybridization.

II. EXPERIMENTAL DETAILS

In order to study the development of the magnetic state in the $UCo_{1-x}Ru_xGe$ system we have prepared a series of polycrystalline samples with different Ru concentrations x between 0 and 0.9. All samples were prepared by arc melting of the stoichiometric amounts of the elements (purity of Co 4N5, Ge 6N, and Ru 3N5). U was purified by the solid state electrotransport technique [27] following previous experience with preparation of UCoGe [27]. The arc-melting process was realized under protective Ar (6N purity) atmosphere on a water-cooled Cu crucible. Each sample was three times turned upside down and subsequently remelted in order to achieve the best homogeneity. All samples were separately wrapped into a Ta foil (99.99%), sealed in a quartz tube under the vacuum of 1×10^{-6} mbar, subsequently annealed at 885 °C for 14 days and then slowly cooled down to room temperature to avoid creation of the internal stresses. Each sample was characterized by x-ray powder diffraction (XRPD) at room temperature on a Bruker D8 Advance diffractometer. The obtained data were evaluated by Rietveld technique [28] using FULLPROF/WINPLOTR software [29,30] with respect to the previously published crystallographic data of the UCoGe [31] and URuGe [24] compound. The chemical composition of our samples was verified by a scanning electron microscope Tescan Mira I LMH equipped with an energy dispersive x-ray detector Bruker AXS. Samples were afterward properly shaped for individual measurements with a fine wire saw to prevent induction of additional stresses and lattice defects. The electrical resistivity (ρ) was measured by the four-probe method on bar-shape samples ($1 \times 0.5 \times 4\,mm^3$) and heat-capacity ($C_p$) measurements were performed on thin plates ($2 \times 2 \times 0.2\,mm^3$) by the relaxation method on PPMS9T and PPMS14T devices using a ^{3}He insert. Magnetization (M) measurements were done on cubic samples ($2 \times 2 \times 2\,mm^3$) using a MPMS7T device. The magnetization was evaluated in μ_B/f.u. For simplicity we omit "/f.u." everywhere throughout the paper.

The electronic structure calculations were performed on the basis of the density-functional theory within the local-spin-density approximation [32] and the generalized gradient approximation [33]. For these calculations we have used the full-potential augmented-plane-wave together with the local-orbitals method (APW+lo) as a part of the latest version (WIEN2K) of the original WIEN code [34].

III. RESULTS

A. X-ray diffraction

Both UCoGe and URuGe crystallize in the orthorhombic TiNiSi-type structure (space group *Pnma*) [24,31] with the room-temperature cell parameters $a = 6.852$ Å, $b = 4.208$ Å, $c = 7.226$ Å and $a = 6.678$ Å, $b = 4.359$ Å, $c = 7.539$ Å, respectively [24,31]. The unit cell volume of UCoGe ($V = 208.3$ Å^3) [31] is about 5% smaller than that of the URuGe compound ($V = 219.5$ Å^3) [24]. The XRPD patterns confirmed the orthorhombic TiNiSi-type structure of samples over the entire concentration range of the $UCo_{1-x}Ru_xGe$ series.

TABLE I. The lattice parameters and the unit cell volume of the $UCo_{1-x}Ru_xGe$ samples as obtained from the refinement of the x-ray powder diffraction patterns.

x	a (Å)	b (Å)	c (Å)	V (Å^3)
0.10	6.8344	4.2188	7.2717	209.6671
0.20	6.8216	4.2267	7.3048	210.6173
0.21	6.8204	4.2261	7.3026	210.4879
0.22	6.8189	4.2279	7.3079	210.6840
0.23	6.8178	4.2272	7.3085	210.6325
0.24	6.8131	4.2280	7.3145	210.6999
0.25	6.8150	4.2320	7.3229	211.2003
0.26	6.8269	4.2385	7.3347	212.2355
0.27	6.8203	4.2363	7.3314	211.8247
0.28	6.8205	4.2390	7.3392	212.1890
0.29	6.8133	4.2373	7.3389	211.8711
0.30	6.8077	4.2373	7.3413	211.7662
0.40	6.7880	4.2454	7.3704	212.3984
0.50	6.7709	4.2577	7.4046	213.4669
0.60	6.7522	4.2710	7.4416	214.6050
0.70	6.7336	4.2868	7.4741	215.7451
0.80	6.7137	4.3015	7.5041	216.7105
0.90	6.6909	4.3212	7.5290	217.6849

The evaluated lattice parameters are listed in Table I. The concentration dependence of all three lattice parameters and the unit volume reveals a linear behavior, i.e., obeying Vegard's law [35] (see Fig. 1).

While the lattice parameters b and c increase with increasing x, the lattice parameter a simultaneously decreases. The volume expansion seems to reflect the increase of the covalent radii from Co (126 pm) to Ru (146 pm) [36]. Refinement of the diffraction patterns showed that the Ru atoms really substitute the Co ones on their sites.

Although the unit cell volume expands with increasing Ru concentration, the distance between the nearest-neighbor U ions $d_{U\text{-}U}$ contracts (see Fig. 1). This result is not surprising because the $d_{U\text{-}U}$ lines form a chain meandering along the a axis.

B. Magnetization and ac susceptibility

We have measured the magnetization of each sample as a function of temperature and applied magnetic field. The values of M_S have been estimated from the magnetization curves measured at 1.85 K (the lowest available temperature in our MPMS7T) by extrapolating the magnetization from high magnetic fields to 0 T.

The values of T_C have been determined by several methods. Arrott plot analysis of magnetization data is widely considered as the most reliable method [37]. For this purpose the

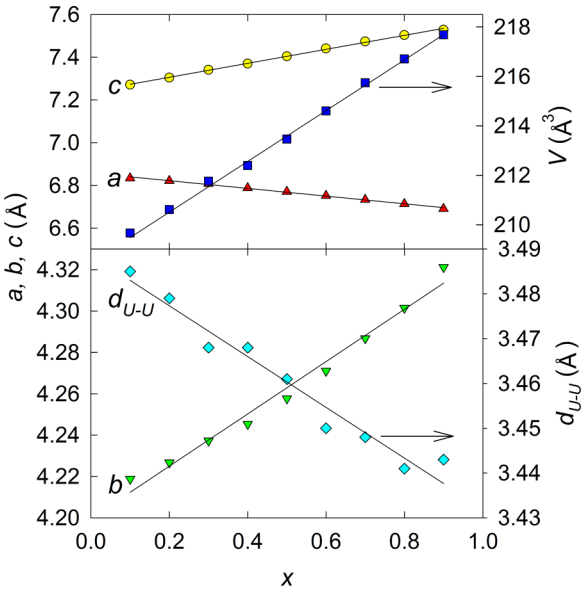

FIG. 1. (Color online) Concentration dependence of the lattice parameters and the unit cell volume of the $UCo_{1-x}Ru_xGe$ samples. The lines serve as guides to the eye.

magnetization curves were measured at several temperatures in the vicinity of the expected T_C. The Arrott plots obtained from our magnetization data are strongly nonlinear. These curves can be approximated by a third degree polynomial function (see a model example in Fig. 2). T_C is determined as the temperature of the Arrott plot isotherm that would cross the M^2 axis at 0. An example of the relevant construction is shown in the inset of Fig. 2.

The nonlinearity of the Arrott plots (the cubic M^2 vs H/M dependence) suggests the presence of a magnetization component linearly dependent on the magnetic field. This is related to the fact that UCoGe and the other UTX compounds crystallizing in the orthorhombic TiNiSi-type structure exhibit strong uniaxial anisotropy with easy magnetization direction along the c axis. The hard magnetization directions within the a-b plane are characteristic by a weak temperature-

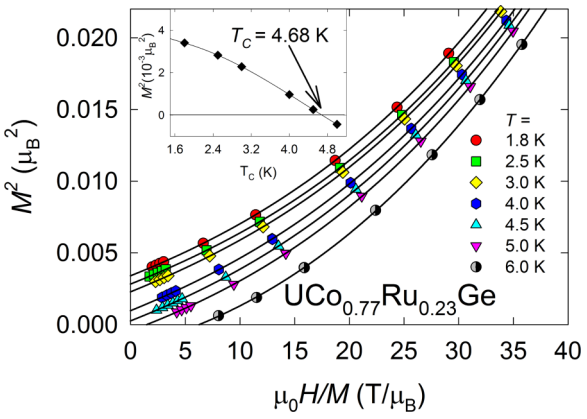

FIG. 2. (Color online) Arrott plots for the $UCo_{0.77}Ru_{0.23}Ge$ compound. Solid lines are the third-order polynomial functions. The inset shows that T_C is taken as the value for which the intersection with the M^2 axis would be zero.

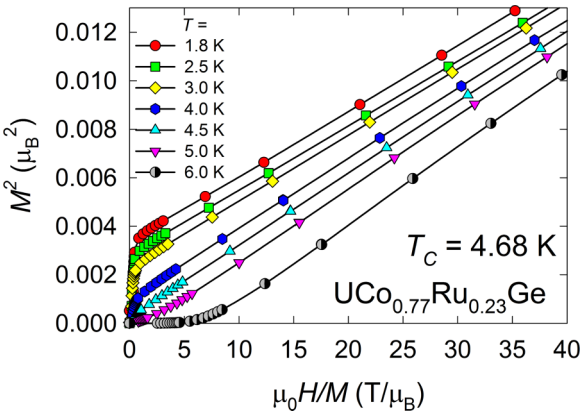

FIG. 3. (Color online) Revised Arrott plots after subtraction of the linear term with the slope $a = 0.006\mu_B\,T^{-1}$ from the magnetization data measured on the $UCo_{0.77}Ru_{0.23}Ge$ sample.

independent paramagnetic response with the magnetization proportional to the magnetic field. We have observed the same type of magnetocrystalline anisotropy for the FM $UCo_{1-x}Ru_xGe$ single crystals which we have grown as a part of another study (see Ref. [38]). Consequently the polycrystalline samples should show a corresponding linear component also in the FM state. By subtracting a suitable linear term from measured magnetization data we obtain the corrected magnetization values $M^* = M - a\mu_0 H$. For $a = 0.006\mu_B\,T^{-1}$ the Arrott plots M^2 vs H/M^* are indeed linear except the low-field part due to low-field magnetization processes and the influence of a demagnetization field as can be seen, for example, in the case of the $UCo_{0.77}Ru_{0.23}Ge$ sample in Fig. 3.

The obtained T_C and M_S values are listed for all samples in Table II and plotted in the complex phase diagram in Fig. 9(a). T_C steeply increases with the initial Ru substitutions for Co, which is in agreement with the results published in previous work [23]. This trend terminates at $x_{max} \approx 0.1$ where the ordering temperature reaches a maximum value of $T_{C,max} \approx 8.6$ K. This value is almost three times higher than $T_C = 3$ K of the parent compound [4] and is comparable with the value found by Huang *et al.* in the case of the corresponding substitution of Fe for Co in UCoGe [39]. Increasing Ru concentration beyond $x \approx 0.1$ is accompanied by a simultaneous decrease of T_C and M_S towards zero at the critical concentration $x_{cr} \approx 0.31$. Thus, the FM dome of the concentration dependence of T_C in the $T - x$ magnetic phase diagram is intimately connected with a corresponding change of M_S [see Fig. 9(a)].

The $M(T)$ curves measured on selected samples with concentration above $x \geqslant 0.1$ displayed in Fig. 4 also manifest the collapse of FM with increasing Ru content. The estimated T_C values as derived from the temperature of the inflection point in the $M(T)$ dependence (measured in low external field of 10 mT are in good agreement with ordering temperatures obtained from the Arrott plot analysis [see Table II and Fig. 9(a)].

We have also measured the ac magnetic susceptibility (χ) for different Ru concentrations above $x \geqslant 0.21$ at temperatures down to 1.85 K using a MPMS device. For measurements

TABLE II. Values of the spontaneous magnetization M_S and Curie temperature derived from the Arrott plot analysis ($T_{C,Arrott}$), temperature dependence of ac susceptibility ($T_{C,\chi}$), magnetization ($T_{C,M}$), and specific heat (T_{C,C_p}), and Sommerfeld coefficient (γ) as determined from the specific-heat data at low temperatures for samples with various concentrations of Ru (x).

x	M_S (μ_B)	$T_{C,Arrott}$ (K)	$T_{C,\chi}$ (K)	$T_{C,M}$ (K)	T_{C,C_p} (K)	γ ($\frac{mJ}{mol\,K^2}$)
0	0.0300	-	-	2.50	-	-
0.01	0.0330	4.20	-	4.00	-	-
0.05	0.0750	8.30	-	7.50	-	-
0.10	0.1060	8.62	-	8.20	8.60	0.0861
0.20	0.0540	5.70	-	5.40	5.70	0.1066
0.21	0.0580	5.70	5.20	5.40	5.90	0.1100
0.22	0.0594	5.01	4.70	5.00	5.30	0.1133
0.23	0.0568	4.68	4.20	4.60	4.30	0.1152
0.24	0.0270	3.55	3.50	3.60	3.80	0.1258
0.25	0.0300	3.49	3.40	3.40	3.30	0.1333
0.26	0.0213	2.51	2.80	2.80	3.00	0.1353
0.27	0.0223	2.77	2.40	2.60	2.80	0.1435
0.28	0.0219	2.32	1.90	2.30	2.70	0.1405
0.29	0.0077	-	1.44	-	1.40	0.1529
0.30	0.0013	-	$\approx$0.35	-	-	0.1598
0.40	0.0011	-	-	-	-	0.1523
0.50	0.0001	-	-	-	-	0.1490

at lower temperatures (down to 400 mK) a custom-made coil system attached to the ^{3}He insert in PPMS and a lock-in amplifier were utilized (the same setup as that used in Ref. [40]). T_C is usually identified as the temperature of the maximum of the real part of χ (see Fig. 5). While the low-temperature ac susceptibility of the sample with $x = 0.29$ reveals a well-developed peak at 1.44 K indicating the onset of FM, no clear peak maximum is observed for the sample with $x = 0.30$, which might be at approximately 350 mK as the lowest-T point was measured at 400 mK. For the sample with $x = 0.31$ no trace of χ anomaly has been detected down to 400 mK, which seems to be in the immediate vicinity of the critical Ru concentration for the existence of FM in the $UCo_{1-x}Ru_xGe$ compounds.

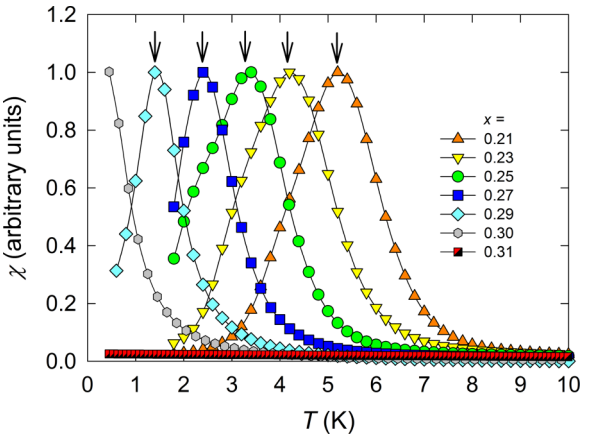

FIG. 5. (Color online) Temperature dependence of the real part of the ac susceptibility of selected $UCo_{1-x}Ru_xGe$ compounds. The arrows mark T_C for each composition. Data are plotted in arbitrary units and normalized because the homemade coil for measurement in ^{3}He (used for measurement of samples with $x = 0.29$–0.31) provides only relative data. Some curves are not shown for clarity of the figure.

C. Specific heat

To analyze the different contributions to the specific heat we have subtracted from experimental data the phonon contribution using the fit of the phonon specific heat as a $C_{ph}(T) = \beta T^3$. We typically obtain values of $\beta \approx (0.52$–$0.56) \times 10^{-3}\,J\,mol^{-1}\,K^{-4}$ which correspond to Debye-temperature values of 151–155 K. The remaining part of the specific heat C represents the sum of the electronic and magnetic contributions C_e and C_m, respectively.

Figure 6 displays the specific heat C divided by temperature T versus T on a log scale for selected samples between $x = 0.1$ and 0.31. The anomaly at T_C is gradually smeared out and shifted to lower temperatures with increasing Ru concentration. Samples with $x \leqslant 0.3$ show clear anomalies that are coincident with the onset of FM order and are

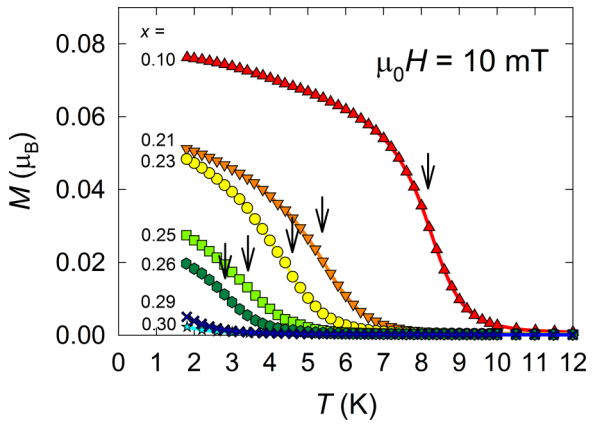

FIG. 4. (Color online) Temperature dependence of the magnetization of selected $UCo_{1-x}Ru_xGe$ compounds measured in an external magnetic field of 10 mT. The arrows mark T_C for each composition.

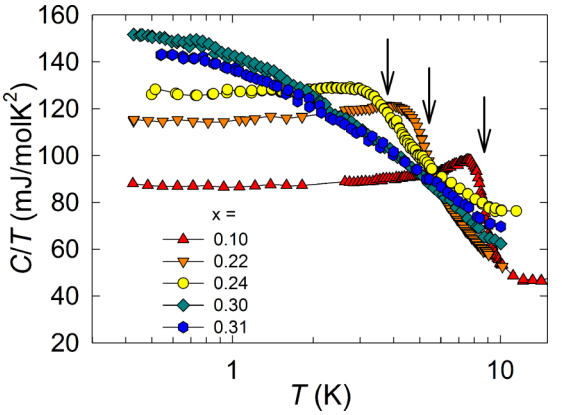

FIG. 6. (Color online) C/T versus log$T$ plot for selected $UCo_{1-x}Ru_xGe$ compounds. Black arrows indicate T_C for samples with $x = 0.10$, 0.22, and 0.24, respectively.

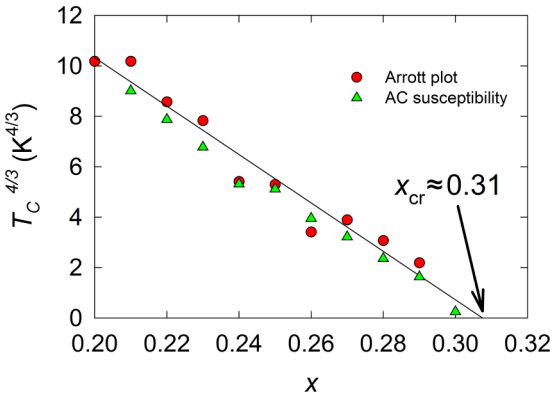

FIG. 7. (Color online) Estimation of the critical concentration for FM in the $UCo_{1-x}Ru_xGe$ system by applying the $T_C^{4/3}$ vs x plot and the T_C values derived from the Arrott plots.

in reasonable agreement with the T_C values derived from magnetization and ac susceptibility [see Table II and Fig. 9(a)]. For samples with $x = 0.30$ and 0.31 C/T versus $\log T$ exhibits nearly linear dependence between 1 and ~ 10 K but gradually levels off at lower temperatures. This indicates a non-Fermi-liquid (NFL) behavior $C(T)/T = c \ln(T_0/T)$ [41,42] that is expected for concentrations in the vicinity of the FM QCP. We note that our data do not follow this dependence in the whole temperature range similar to that recently reported on the $UCo_{1-x}Fe_xGe$ system [39].

We further calculate the magnetic entropy S_m integrated over the temperature range from 0.7 K up to the T_C for each sample and find a steady decrease of S_m with increasing x from $0.13R \ln 2$ for $x = 0.1$ down to $0.006R \ln 2$ at $x = 0.30$ [see Fig. 9(c)]. This is consistent with the observation of a gradual disappearance of the itinerant magnetic moment by approaching the QCP ($x_{cr} \approx 0.31$). As the system approaches the critical concentration we observe a large increase of the value of Sommerfeld coefficient γ with a maximum near $x_{cr} \approx 0.31$ which reflects an enhancement of the effective mass of the quasiparticles in the region where FM is suppressed. This finding is consistent with the presence of a strong spin fluctuation near the FM QCP. According to the prediction for the dependence of T_C on a control parameter (x) for itinerant FM QCP by Millis and Hertz [41,42] the ordering temperature should obey the relation $T_C \sim (x_{cr} - x)^{3/4}$ [43], i.e., a linear $T_C^{4/3}$ vs x plot. As we show in Fig. 7 a linear fit of T_C values for the samples with x from 0.2 to 0.3 reveals that T_C vanishes at the critical concentration $x_{cr} \approx 0.31$ consistent with this model.

D. Electrical resistivity

The low-temperature resistivity data measured on selected polycrystalline samples are plotted in Fig. 8. Anomalies connected with the transition from a paramagnetic to a FM state are not clearly visible. It is evident, that increasing Ru content leads to considerable changes of the low-temperature resistivity behavior. The $\rho(T)$ data below T_C reasonably follow the $\rho = \rho_0 + AT^2$ dependence usual for FMs. Data above T_C

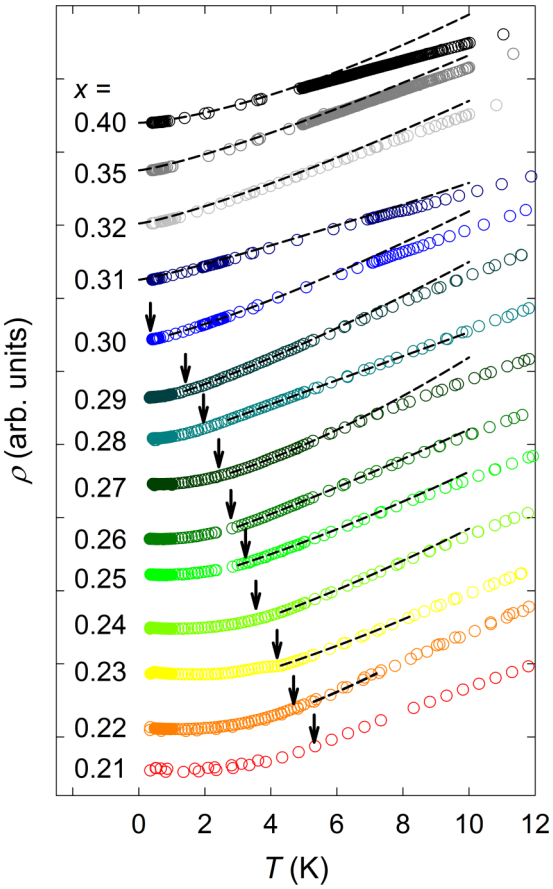

FIG. 8. (Color online) Temperature dependence of the electrical resistivity for selected polycrystalline samples of $UCo_{1-x}Ru_xGe$. The vertical arrows denote T_C values obtained from ac susceptibility data. Dashed lines are fits to data above T_C according to Eq. (1). Each curve is arbitrarily vertically shifted for better clarity of the figure.

were fitted to the relation

$$\rho = \rho_0 + AT^n. \quad (1)$$

The inflection point of the $\rho(T)$ dependence was taken as an upper limit for the fitting. The exponent (n) gradually decreases as the Ru content approaches the critical concentration x_{cr}. The minimum value of $n \approx 1.13$ for $x = 0.31$ is close to the proposed linear temperature dependence from the theory of Millis and Hertz [41–43] for NFL behavior of a clean three-dimensional itinerant FM rather than to the scaling with the exponent $n = 5/3$ which follows from the spin-fluctuation theory of Moriya [43]. The samples with higher concentration of Ru ($x > x_{cr}$) seem to exhibit gradual recovery towards a FL state which is documented by increasing the value of n exponent with increasing x above x_{cr}.

Development of the exponent n is summarized in the $T - x$ phase diagram [Fig. 9(b)]. In order to see the exponent n as a function of temperature we have calculated the logarithmic derivative of the electrical resistivity according to Eq. (2):

$$n = \frac{d \ln(\rho - \rho_0)}{d \ln T}. \quad (2)$$

The results of this analysis are displayed in the colored part of the phase diagram in Fig. 9(a). One can see a significant

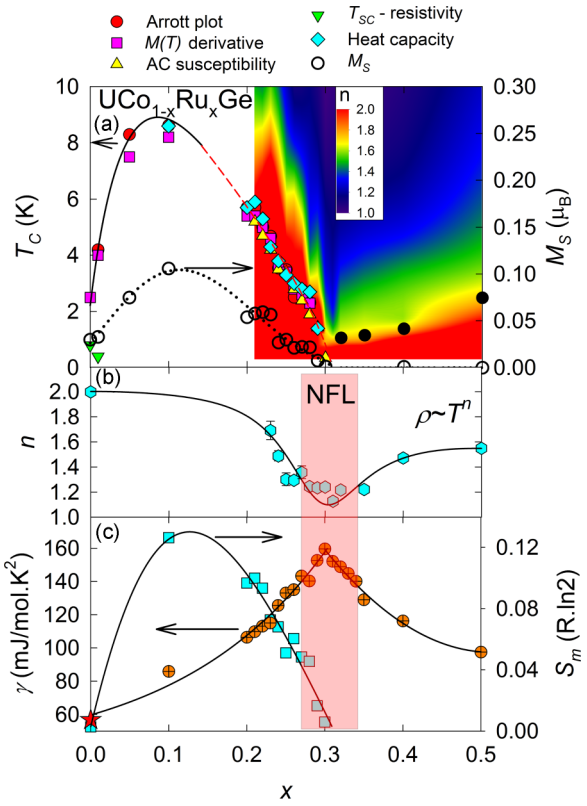

FIG. 9. (Color online) Panel (a) shows the $T - x$ phase diagram based on measurements of polycrystalline samples. The diagram is supplemented by the results of the electrical resistivity measurement revealing the occurrence of SC in the parent UCoGe compound and in $UCo_{0.99}Ru_{0.01}Ge$—the two data points are taken from Ref. [23] (green triangle). The black solid line is only a guide to the eye, while the red dashed part is a fit of $T_C \sim (x_{cr} - x)^{3/4}$. The right axis denotes the spontaneous magnetization M_S (dashed line in the plot is only a guide to the eye). The color plot shows local exponents of the resistivity obtained as $n = \frac{d \ln(\rho - \rho_0)}{d \ln T}$. The black filled circles show the temperature where resistivity starts to deviate from the T^2 dependence. Panel (b) shows the evolution of the coefficients n from the fitting of the low-temperature dependence of the electrical resistivity with equation $\rho = \rho_0 + AT^n$ for $T > T_C$. The right vertical axis shows $\mathrm{RRR} = \rho_{300\,\mathrm{K}}/\rho_{0.4\,\mathrm{K}}$ as a function of x. Panel (c) shows the development of C/T (extrapolated to 0 K) and the magnetic entropy S_m (value for the parent UCoGe is taken from Ref. [44] and is marked by a star).

change of the exponent between the region of FM ordering ($T < T_C$) where $n = 2$ and in the nonmagnetic state where $n < 2$. The sharp decrease of the value n near x_{cr} down to the lowest temperatures is surrounded by regions of higher n (rapidly increasing on the FM side for $x < x_{cr}$ and slower increase on the paramagnetic side).

E. Theoretical calculations

In order to better understand the changes in the electronic structure of the $UCo_{1-x}Ru_xGe$ compounds across the ferromagnetic QCP, we have performed first-principles theoretical calculations on the paramagnetic compound URuGe. As a matter of fact, while the density of states (DOS) of the parent

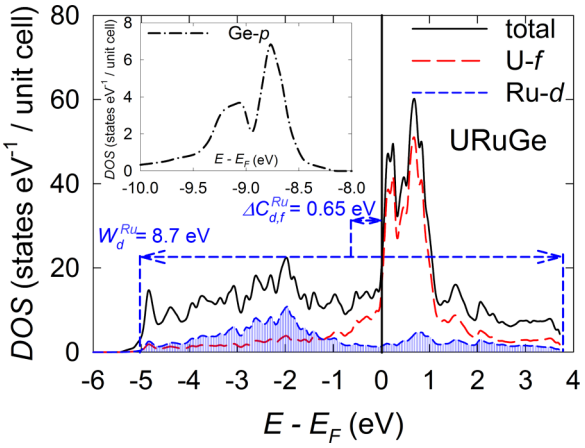

FIG. 10. (Color online) Total and partial DOS for U-f states and Ru-d states in URuGe. Width of the d band (W_d^{Ru}) and its center $\Delta C_{df}^{\mathrm{Ru}}$ are marked by dashed arrows. The inset shows that the contribution of the Ge-p states is far from the Fermi level.

compound UCoGe is known (Ref. [45]) the information about the DOS of URuGe is missing. The calculated total and partial DOS of the URuGe are plotted in Fig. 10.

We used the calculated URuGe band structure by considering the simple model of Silva Neto *et al.* [46] which is based on the periodic Anderson model [47,48]. This simplified model proposes the key role of the nd-5f hybridization [V_{df} in Eq. (3)], where n is the number of d electrons in the observed nonmonotonous evolution of T_C in the $URh_{1-x}Co_xGe$ system. They described the evolution of T_C with increasing x as a consequence of the broadening of the nd and 5f bands (W_d, W_f), respectively, and the mutual shift of their centers ($C_{Td} - C_{Uf}$) that are related as [46]

$$V_{df} = \frac{W_d W_f}{C_{Td} - C_{Uf}}. \tag{3}$$

If we apply this model to our $UCo_{1-x}Ru_xGe$ system we can qualitatively describe the nonmonotonous evolution of T_C with Ru concentration. The concentration dependence of the broadness of the nd band is assumed to be linear according to Eq. (4):

$$W_d(x) = W_d^{\mathrm{Co}}(1 - x) + W_d^{\mathrm{Ru}}(x), \tag{4}$$

where $W_d^{\mathrm{Co}} = 6.1$ eV (Ref. [45]) and $W_d^{\mathrm{Ru}} = 8.7$ eV (see Fig. 10) and $W_f = 0.43$ eV (Ref. [45]). Such a behavior is consistent with other UTX (T = transition metal, X = p element) compounds where the d band broadens while we move from the 3d to the 4d transition metals [49]. Consequently $(C_{Td} - C_{Uf})(x) = \Delta C_{df}(x)$ deviates from linearity

$$\Delta C_{df}(x) = \Delta C_{df}^{\mathrm{Co}}(1 - x) + \Delta C_{df}^{\mathrm{Ru}}(x) + \delta' x^2(1 - x) + \delta'' x(1 - x)^2. \tag{5}$$

We used the values from calculated DOSs, i.e., $\Delta C_{df}^{\mathrm{Ru}} = 0.65$ eV and $\Delta C_{df}^{\mathrm{Co}} = 1.5$ eV (Ref. [45]) and adjustable parameters were taken as $\delta' = 2 \times 10^{-5}$ and $\delta'' = 2$. Such an approach leads to a nonmonotonous dependence of the d-f hybridization term V_{df}; starting with $V_{df}(x = 0) \approx 1.73$ for UCoGe (in agreement with Ref. [46]), $V_{df}(x = 1) \approx 5.55$

for URuGe and $V_{df}(x \approx 0.3) \approx 1.9$ as estimated for the FM QCP [46]. The overall $V_{df}(x)$ dependence starts with its decrease and thereby causes an enhancement of the density of f states at the Fermi level $N_f(E_F)$ [50]. In the case of itinerant FMs we can estimate the ordering temperature as a function of the density of states at the Fermi level $T_C \sim [IN(E_F) - 1]^{3/4}$ where I is the Stoner integral and $N(E_F)$ is the total density of states at the Fermi level [51]. In this respect we can attribute the initial increase of T_C to the enhanced $N(E_F)$. At $x \approx 0.07$ the d-f hybridization reaches its minimum value $V_{df} = 1.7$ and starts to increase with increasing x. This point qualitatively corresponds to the position of the maximum T_C in the experimental data at $x \approx 0.1$. As the Ru concentration increases the d band is shifted closer to the position of the f band and the hybridization increases and thereby results in a reduction of the contribution of the $N_f(E_F)$ to $N(E_F)$ [50]. For the reason mentioned above the ordering temperature decreases and reaches zero near $x_{cr} \approx 0.31$.

IV. DISCUSSION

The $5f$-electron magnetism in uranium compounds is controlled by the degree of overlap of the $5f$ wave functions of neighboring U ions and by the hybridization of the U-ion $5f$-electron states with states of the ligand valence electrons ($5f$-ligand hybridization). These two mechanisms cause the $5f$-electron orbitals to lose their atomic character which they exhibit in the U free ion. Thus, the $5f$-$5f$ overlap and/or strong $5f$-ligand hybridization lead to delocalization of the $5f$ electrons, their participation in metallic bonding [52], and consequently a washout of the U magnetic moment [53]. In addition, the spin-orbit interaction in the U ion plays an important role in electronic structure. Accordingly, an orbital magnetic moment antiparallel to the spin moment is induced by the strong spin-orbit coupling in the spin-polarized energy bands of itinerant $5f$-electron materials [54,55]. The magnitude of the U $5f$-electron magnetic moments is thus further strongly reduced due to the mutual compensation of the orbital and spin components. The orbital moment is by rule larger than the spin moment considering results of so far done relevant experiments (see relevant references in Ref. [56]).

On the other hand, the $5f$-ligand hybridization plays a dual role in U compounds. Besides washing out the $5f$-electron magnetic moment it mediates an indirect exchange interaction which couples the uranium magnetic moments to promote the magnetic ordering and simultaneously causes very strong magnetocrystalline anisotropy even in very weak itinerant magnets [56,57]. Within this process the hybridized ligand valence states become polarized and as a result the ligand ion (especially the transition element ion) exhibits a small induced magnetic moment which is usually parallel to the dominant $5f$-electron orbital component (see relevant references in Ref. [56]). This scenario apparently holds for UCoGe as evidenced from a recent x-ray magnetic circular dichroism study [58] and polarized neutron diffraction experiments on $UCo_{0.97}Ru_{0.03}Ge$ and $UCo_{0.88}Ru_{0.12}Ge$ single crystals [38]. These experiments confirm that the $5f$-electron orbital moment dominates the antiparallel spin component. A much smaller Co magnetic moment is induced by the $5f$-$3d$ hybridization.

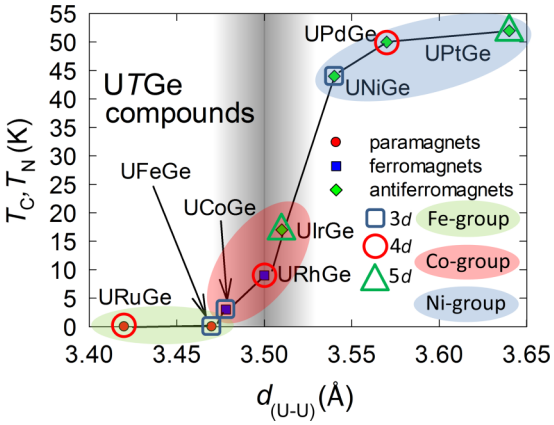

FIG. 11. (Color online) Illustrative plot showing the dependence of the ordering temperature of the UTGe compounds (T = transition metal) on the shortest distance between two nearest uranium atoms (d_{U-U}). The shaded region spreads around Hill limit (3.5 Å) [59] valid for uranium. The position of UFeGe is exceptional because UFeGe does not keep the TiNiSi-type structure [31].

Considering the change of the U-U distance d_{U-U} between the nearest U neighbor ions (overlap of $5f$ orbitals) within the $UCo_{1-x}Ru_xGe$ series, we find that d_{U-U} decreases with increasing Ru concentration from ≈3.48 Å in UCoGe to 3.44 Å in URuGe (see Figs. 1 and 11). Both values fall rather on the "nonmagnetic side" of the Hill plot [59]. On the other hand, one should bear in mind that each U ion has only two nearest U neighbors on the d_{U-U} chain meandering along the a axis. If the $5f$-$5f$ overlap was the only mechanism controlling magnetism, then a gradual washout of U magnetic moment and monotonous decreasing of T_C with increasing Ru content would be expected. On the contrary, however, we observe an initial rapid increase of T_C to a maximum followed by a suppression of FM with further increasing x. We note that our observation of a FM dome in magnetic phase diagram in $UCo_{1-x}Ru_xGe$ [see Fig. 9(a)] is similar to those observed for $UCo_{1-x}Fe_xGe$ [39], $URh_{1-x}Ru_xGe$ [26], and $URh_{1-x}Co_xGe$ [25].

Apparently an additional mechanism, namely, the $5f$-ligand hybridization, must be taken into account for conceiving the complex evolution of FM in these systems. The increase of T_C and U magnetic moment with increasing x up to 0.12 is accompanied by increasing the $5f$-electron orbital moment [38]. The increase of the orbital moment is usually considered as a sign of partial localization of $5f$ electrons because the orbital moment density is distributed closer to the nucleus than the spin density as has been demonstrated on a detailed study of the U $5f$-electron form factor in UFe_2 [55,60]. Nevertheless, the μ_L/μ_S ratio of ≈2.3 indicates still a significant delocalization of the $5f$-electron states for $x = 0.12$ [38]. As we mention above our theoretical band structure calculation provides the basis for understanding the mechanism responsible for the FM dome in the magnetic phase diagram of $UCo_{1-x}Ru_xGe$ by following the simple model treating the changes of $5f$-nd hybridization with variations of the widths and mutual positions on the energy scale of the transition metal d bands and U $5f$ bands [46]. Accordingly, the nonisoelectronic substitution of

Co by Ru causes broadening of the d band from $3d$ to $4d$ transition-metal-like. Together with the mutual movement of the d and f bands on energy scale itself we can qualitatively conceive the domelike dependence of the ordering temperature T_C. This is an important confirmation of the trend. Variations of the $5f$-nd hybridization most likely cause analogous nonmonotonous variation of the magnetic ground state of $UCo_{1-x}Fe_xGe$ [39] and $URh_{1-x}Ru_xGe$ [26] exhibiting also a FM dome in the magnetic phase diagram. It is worth mentioning that the nonmonotonous evolution of magnetic ground state causing a FM dome in the magnetic phase diagram is not only specific to the $UTGe$ compounds possessing the orthorhombic TiNiSi-type structure. Analogous trends reflecting the varying $5f$-nd hybridization are observed also in UTX compounds with the hexagonal ZrNiAl-type structure. Here UFeAl [61], URuAl [62], and UCoAl [63] are paramagnets. The latter compound is, however, close to a FM instability. A magnetic field of only 0.6 T induces in UCoAl itinerant electron metamagnetism [64,65]. URhAl [62] and URhGe [56] are FMs. FM domes are observed in the magnetic phase diagrams of $UCo_{1-x}Ru_xAl$ [66], $URh_{1-x}Ru_xAl$ [67], and $URh_{1-x}Ru_xGa$ [67] and anticipated from the results reported on $UCo_{1-x}Fe_xAl$ [68].

The observed strong delocalization of the $5f$ electrons in $UCo_{1-x}Ru_xGe$ at higher Ru concentrations is reflected by a dramatic decrease of the magnetic entropy S_m down to the $0.006R\ln 2$ for $x = 0.30$ which points to the itinerant nature of the weak FM in the vicinity of the critical concentration. Note that a magnetic entropy equal to zero is expected for an ideal itinerant electron FM [56]. Our results of the temperature dependence of the electrical resistivity provide evidence for a NFL behavior in the vicinity of x_{cr} most likely caused by the possible presence of the FM QCP. We have observed a drop of the n exponent in the temperature dependence of resistivity $\rho = \rho_0 + AT^n$ and an almost logarithmic dependence of the heat capacity $C(T)/T = c\ln(T_0/T)$ in a limited interval at lowest temperatures that would be in agreement with the theoretical predictions of Millis and Hertz [41,42]. Further evidence for the FM QCP is offered by the rapid increase of the effective mass of the quasiparticles near x_{cr}. The proposed scenario is also corroborated by scaling of the ordering temperature with the control parameter itself which obeys the formula $T_C \sim (x_{cr} - x)^{3/4}$ and provides estimation of the critical concentration $x_{cr} \approx 0.31$.

The FM transition of $UCo_{1-x}Ru_xGe$ compounds in the vicinity of x_{cr} is apparently of a second-order type in contrast to the first-order transition reported for three-dimensional FMs in the vicinity of a QCP [69]. Microscopic nuclear quadrupole resonance studies of UCoGe suggest a first-order transition to the FM state [70]. The second-order transition in $UCo_{1-x}Ru_xGe$ compounds near x_{cr} can be conceived as a consequence of the substitution-induced disorder in the system which may blur the first-order transition towards a continuous second-order transition. In this context, we would like to mention the experimental and theoretical arguments regarding the observed anomalies related to the existence of a FM QCP in $UCo_{1-x}Ru_xGe$ should be considered with proper caution. Disorder caused by substitution can in some cases emulate NFL behavior [71,72] and may be one of the reasons for the lacking SC in $UCo_{1-x}Ru_xGe$ in the proximity of the QCP. Thorough investigation of single crystals of $UCo_{1-x}Ru_xGe$ compounds near x_{cr} at ambient and high pressures is highly desired in order to clarify the origin of the NFL state and the character of the FM QPT in $UCo_{1-x}Ru_xGe$.

V. CONCLUSIONS

We have successfully prepared a series of polycrystalline samples of UCoGe doped with Ru in a wide range of concentration $UCo_{1-x}Ru_xGe$ ($0 \geqslant x \leqslant 0.9$). The Ru substitution leads to the development of a FM dome between $x = 0$ and 0.31 with the maximum of $T_C = 8.6$ K and $M_S = 0.1\mu_B$ appearing at $x \approx 0.1$. Further increase of the Ru content up to the critical concentration $x_{cr} \approx 0.31$ leads to the disappearance of the FM state at a QCP. Using electronic structure calculations we were able to explain the evolution of FM with x for $UCo_{1-x}Ru_xGe$ in terms of changes of the density of states at the Fermi level due to varying $5f$-ligand hybridization. The analysis of the critical exponents of the electrical resistivity and heat capacity at low temperatures revealed a non-Fermi-liquid behavior for the samples in the vicinity of the QCP. The NFL state can be influenced by the substitution-induced disorder of the system because of the nonisoelectronic mixture of the $3d$ (Co) and $4d$ (Ru) bands. Further study of the region around the critical concentration including the measurements under the external pressure performed on high-quality single crystals is highly desired for a better understanding the physics underlying the FM QPT.

ACKNOWLEDGMENTS

This work was supported by the Czech Science Foundation Grant No. P204/12/P418 and the Charles University in Prague, project GA UK No. 720214. Experiments performed in MLTL [73] were supported within the program of Czech Research Infrastructures (Project No. LM2011025).

[1] S. S. Saxena, P. Agarwal, K. Ahilan, F. M. Grosche, R. K. W. Haselwimmer, M. J. Steiner, E. Pugh, I. R. Walker, S. R. Julian, P. Monthoux, G. G. Lonzarich, A. Huxley, I. Sheikin, D. Braithwaite, and J. Flouquet, Nature (London) **406**, 587 (2000).

[2] A. Huxley, I. Sheikin, E. Ressouche, N. Kernavanois, D. Braithwaite, R. Calemczuk, and J. Flouquet, Phys. Rev. B **63**, 144519 (2001).

[3] D. Aoki, A. Huxley, E. Ressouche, D. Braithwaite, J. Flouquet, J.-P. Brison, E. Lhotel, and C. Paulsen, Nature (London) **413**, 613 (2001).

[4] N. T. Huy, A. Gasparini, D. E. de Nijs, Y. Huang, J. C. P. Klaasse, T. Gortenmulder, A. de Visser, A. Hamann, T. Gorlach, and H. von Lohneysen, Phys. Rev. Lett. **99**, 067006 (2007).

[5] M. Uhlarz, C. Pfleiderer, and S. M. Hayden, Phys. Rev. Lett. **93**, 256404 (2004).

[6] D. E. de Nijs, N. T. Huy, and A. de Visser, Phys. Rev. B **77**, 140506(R) (2008).

[7] C. Stock, D. A. Sokolov, P. Bourges, P. H. Tobash, K. Gofryk, F. Ronning, E. D. Bauer, K. C. Rule, and A. D. Huxley, Phys. Rev. Lett. **107**, 187202 (2011).

[8] T. Hattori, Y. Ihara, Y. Nakai, K. Ishida, Y. Tada, S. Fujimoto, N. Kawakami, E. Osaki, K. Deguchi, N. K. Sato, and I. Satoh, Phys. Rev. Lett. **108**, 066403 (2012).

[9] D. v. d. Marel, H. J. A. Molegraaf, J. Zaanen, Z. Nussinov, F. Carbone, A. Damascelli, H. Eisaki, M. Greven, P. H. Kes, and M. Li, Nature (London) **425**, 271 (2003).

[10] C. Pfleiderer, G. J. McMullan, S. R. Julian, and G. G. Lonzarich, Phys. Rev. B **55**, 8330 (1997).

[11] A. Schroder, G. Aeppli, R. Coldea, M. Adams, O. Stockert, H. v. Lohneysen, E. Bucher, R. Ramazashvili, and P. Coleman, Nature (London) **407**, 351 (2000).

[12] H. v. Lohneysen, T. Pietrus, G. Portisch, H. G. Schlager, A. Schroder, M. Sieck, and T. Trappmann, Phys. Rev. Lett. **72**, 3262 (1994).

[13] J. Custers, P. Gegenwart, H. Wilhelm, K. Neumaier, Y. Tokiwa, O. Trovarelli, C. Geibel, F. Steglich, C. Pepin, and P. Coleman, Nature (London) **424**, 524 (2003).

[14] C. Pfleiderer and A. D. Huxley, Phys. Rev. Lett. **89**, 147005 (2002).

[15] D. Belitz, T. R. Kirkpatrick, and T. Vojta, Phys. Rev. Lett. **82**, 4707 (1999).

[16] V. P. Mineev, C. R. Phys. **12**, 567 (2011).

[17] M. Janoschek, M. Garst, A. Bauer, P. Krautscheid, R. Georgii, P. Boni, and C. Pfleiderer, Phys. Rev. B **87**, 134407 (2013).

[18] A. Menovsky, F. R. de Boer, P. H. Frings, and J. J. M. Franse, in *High Field Magnetism*, edited by M. Date (Elsevier, Amsterdam, 1983), pp. 189–191.

[19] M. Sutherland, R. P. Smith, N. Marcano, Y. Zou, S. E. Rowley, F. M. Grosche, N. Kimura, S. M. Hayden, S. Takashima, M. Nohara, and H. Takagi, Phys. Rev. B **85**, 035118 (2012).

[20] D. Aoki and J. Flouquet, J. Phys. Soc. Jpn. **81**, 011003 (2012).

[21] A. Gasparini, Y. K. Huang, N. T. Huy, J. C. P. Klaasse, T. Naka, E. Slooten, and A. de Visser, J. Low Temp. Phys. **161**, 134 (2010).

[22] D. Aoki, T. D. Matsuda, V. Taufour, E. Hassinger, G. Knebel, and J. Flouquet, J. Phys. Soc. Jpn. **78**, 113709 (2009).

[23] J. Pospisil, J. P. Vejpravova, M. Divis, and V. Sechovsky, J. Appl. Phys. **105**, 07E114 (2009).

[24] R. Troc and V. H. Tran, J. Magn. Magn. Mater. **73**, 389 (1988).

[25] N. T. Huy and A. de Visser, Solid State Commun. **149**, 703 (2009).

[26] N. T. Huy, A. Gasparini, J. C. P. Klaasse, A. de Visser, S. Sakarya, and N. H. van Dijk, Phys. Rev. B **75**, 212405 (2007).

[27] J. Pospisil, K. Prokes, M. Reehuis, M. Tovar, J. Poltierova Vejpravova, J. Prokleska, and V. Sechovsky, J. Phys. Soc. Jpn. **80**, 084709 (2011).

[28] H. Rietveld, J. Appl. Cryst. **2**, 65 (1969).

[29] J. Rodriguez-Carvajal, Physica B (Amsterdam, Neth.) **192**, 55 (1993).

[30] T. Roisnel and J. Rodríguez-Carvajal, Materials Science Forum **378–381**, 118 (2001).

[31] F. Canepa, P. Manfrinetti, M. Pani, and A. Palenzona, J. Alloys Compd. **234**, 225 (1996).

[32] J. P. Perdew and Y. Wang, Phys. Rev. B **45**, 13244 (1992).

[33] J. P. Perdew, K. Burke, and M. Ernzerhof, Phys. Rev. Lett. **77**, 3865 (1996).

[34] K. Schwarz, P. Blaha, and G. K. H. Madsen, Comput. Phys. Commun. **147**, 71 (2002).

[35] L. Vegard, Z. Phys. A: Hadrons Nuclei **5**, 17 (1921).

[36] B. Cordero, V. Gomez, A. E. Platero-Prats, M. Reves, J. Echeverria, E. Cremades, F. Barragan, and S. Alvarez, Dalton Trans. (2008) 2832.

[37] A. Arrott, Phys. Rev. **108**, 1394 (1957).

[38] M. Valiska, J. Pospisil, A. Stunault, Y. Takeda, B. Gillon, Y. Haga, K. Prokes, M. M. Abd-Elmeguid, G. Nenert, T. Okane, H. Yamagami, L. Chapon, A. Gukasov, A. Cousson, E. Yamamoto, and V. Sechovsky, J. Phys. Soc. Jpn. (to be published), arXiv:1504.05645.

[39] K. Huang, J. J. Hamlin, R. E. Baumbach, M. Janoschek, N. Kanchanavatee, D. A. Zocco, F. Ronning, and M. B. Maple, Phys. Rev. B **87**, 054513 (2013).

[40] J. Prokleska, J. Pospisil, J. Vejpravova Poltierova, V. Sechovsky, and J. Sebek, J. Phys.: Conf. Ser. **200**, 012161 (2010).

[41] A. J. Millis, Phys. Rev. B **48**, 7183 (1993).

[42] J. A. Hertz, Phys. Rev. B **14**, 1165 (1976).

[43] G. R. Stewart, Rev. Mod. Phys. **73**, 797 (2001).

[44] A. Gasparini, Y. K. Huang, J. Hartbaum, H. von Lohneysen, and A. de Visser, Phys. Rev. B **82**, 052502 (2010).

[45] M. Divis, Physica B (Amsterdam, Neth.) **403**, 2505 (2008).

[46] M. B. S. Neto, A. H. C. Neto, J. S. Kim, and G. R. Stewart, J. Phys.: Condens. Matter **25**, 025601 (2013).

[47] C. D. Batista, J. Bonca, and J. E. Gubernatis, Phys. Rev. Lett. **88**, 187203 (2002).

[48] C. D. Batista, J. Bonca, and J. E. Gubernatis, Phys. Rev. B **68**, 214430 (2003).

[49] T. Gasche, M. S. S. Brooks, and B. Johansson, J. Phys.: Condens. Matter **7**, 9499 (1995).

[50] D. M. Newns and N. Read, Adv. Phys. **36**, 799 (1987).

[51] T. Moriya, *Spin Fluctuations in Itinerant Electron Magnetism* (Springer, Berlin, Heidelberg, 2012).

[52] J. L. Smith and E. A. Kmetko, J. Less-Common Met. **90**, 83 (1983).

[53] B. R. Cooper, Q. G. Sheng, S. P. Lim, C. Sanchez-Castro, N. Kioussis, and J. M. Wills, J. Magn. Magn. Mater. **108**, 10 (1992).

[54] M. S. S. Brooks and P. J. Kelly, Phys. Rev. Lett. **51**, 1708 (1983).

[55] G. H. Lander, M. S. S. Brooks, and B. Johansson, Phys. Rev. B **43**, 13672 (1991).

[56] V. Sechovsky and L. Havela, in *Handbook of Magnetic Materials*, edited by K. H. J. Buschow (Elsevier, New York, 1998), Vol. 11, pp. 1–289.

[57] C. Sanchez-Castro, B. R. Cooper, and K. S. Bedell, Phys. Rev. B **51**, 12506 (1995).

[58] M. Taupin, J.-P. Brison, D. Aoki, J.-P. Sanchez, F. Wilhelm, and A. Rogalev, arXiv:1501.01251.

[59] H. H. Hill, in *Plutonium 1970 and Other Actinides*, edited by W. N. Miner (The Metallurgical Society of AIME, New York, 1970), pp. 2–19.

[60] M. Wulff, G. H. Lander, B. Lebech, and A. Delapalme, Phys. Rev. B **39**, 4719 (1989).

[61] R. Troc, V. H. Tran, F. G. Vagizov, and H. Drulis, J. Alloys Compd. **200**, 37 (1993).

[62] P. A. Veenhuizen, F. R. de Boer, A. A. Menovsky, V. Sechovsky, and L. Havela, J. Phys. **49**, 485 (1988).

[63] O. Eriksson, B. Johansson, and M. S. S. Brooks, J. Phys.: Condens. Matter **1**, 4005 (1989).

[64] M. Shimizu, J. Phys. (Paris) **43**, 155 (1982).

[65] N. V. Mushnikov, T. Goto, K. Kamishima, H. Yamada, A. V. Andreev, Y. Shiokawa, A. Iwao, and V. Sechovsky, Phys. Rev. B **59**, 6877 (1999).
[66] A. V. Andreev, L. Havela, V. Sechovsky, M. I. Bartashevich, J. Sebek, R. V. Dremov, and I. K. Kozlovskaya, Philos. Mag. B **75**, 827 (1997).
[67] V. Sechovsky, L. Havela, F. R. de Boer, P. A. Veenhuizen, K. Sugiyama, T. Kuroda, E. Sugiura, M. Ono, M. Date, and A. Yamagishi, Physica B (Amsterdam, Neth.) **177**, 164 (1992).
[68] N. V. Mushnikov, T. Goto, A. V. Andreev, V. Sechovsky, and H. Yamada, Phys. Rev. B **66**, 064433 (2002).
[69] D. Belitz and T. R. Kirkpatrick, arXiv:1204.0873.
[70] T. Hattori, K. Ishida, Y. Nakai, T. Ohta, K. Deguchi, N. K. Sato, and I. Satoh, Physica C (Amsterdam, Neth.) **470**, S561 (2010).
[71] E. Miranda, V. Dobrosavljevic, and G. Kotliar, Phys. Rev. Lett. **78**, 290 (1997).
[72] A. Rosch, Phys. Rev. Lett. **82**, 4280 (1999).
[73] See http://mltl.eu/.